# Comb-shaped alkyl imidazolium-functionalized poly(arylene ether sulfone)s as high performance anion-exchange membranes

**ARTICLE** · MARCH 2015

DOI: 10.1039/C5TA01123J



**3 AUTHORS**, INCLUDING:

Anil Rao
Korea Institute of Science and Technology
**7** PUBLICATIONS **75** CITATIONS
SEE PROFILE

Sang Yong Nam
Gyeongsang National University
**91** PUBLICATIONS **1,275** CITATIONS
SEE PROFILE

Journal of Materials Chemistry A

PAPER

Cite this: J. Mater. Chem. A, 2015, 3, 8571

# Comb-shaped alkyl imidazolium-functionalized poly(arylene ether sulfone)s as high performance anion-exchange membranes†

Anil H. N. Rao,[a] SangYong Nam[b] and Tae-Hyun Kim*[a]

Received 11th February 2015
Accepted 13th March 2015

DOI: 10.1039/c5ta01123j

www.rsc.org/MaterialsA

Comb-shaped poly(arylene ether sulfone)s with pendant alkyl imidazolium groups were developed as anion-exchange membranes (AEMs). The imidazolium-functionalized polymers with relatively long alkyl chains formed self-aggregated structures with large ionic clusters and clear hydrophilic–hydrophobic phase separation. These comb-shaped membranes, with ion-exchange capacities of only 0.92–1.14 meq $g^{-1}$, showed very high hydroxide conductivities of over 0.03 S $cm^{-1}$ at 20 °C and 0.14 S $cm^{-1}$ at 80 °C. Furthermore, the self-aggregated structure resulting from these comb-shaped polymers exhibited excellent thermal, mechanical and dimensional stability, as well as superior chemical stability at high pH.

## Introduction

The alkaline exchange membrane fuel cell (AEMFC) is considered to be a more promising energy conversion device for stationary and mobile applications than the proton exchange membrane fuel cell (PEMFC) because of its improved oxygen reduction kinetics and better fuel oxidation kinetics. These features can lead to higher efficiencies and enable the use of non-precious metal catalysts, greatly reducing the cost of the device.[1–4]

The anion, *i.e.* $OH^-$, exchange membrane (AEM) is one of the key components of AEMFCs, and should possess certain properties, such as high ionic conductivity, low degree of swelling, and high chemical stability.[5–9] A variety of AEMs, whose main polymer chain structures range from poly(arylene ether)s and their analogues,[6,7] polyimides[8] to poly(phenylene oxide)s[9] have been studied. Among these polymer structures, poly(arylene ether sulfone)s, having the advantages of good solubility, high thermal stability, excellent mechanical properties and versatile chemical modification, have been most widely applied to AEMs by applying a post-functionalization strategy using mainly quaternary ammonium cations as an $OH^-$ conductor. However, quaternary ammonium cations are generally unstable in high pH aqueous solution.[10–12] As potential alternative cations, guanidium,[13] piperazinium,[14] imidazolium,[15–17] morpholinium[18] and metal cations[19] have been investigated. Among the cations studied, imidazolium-based AEMs have recently drawn particular interest due to their relatively high chemical stability, which is largely attributed to the steric hindrance and the presence of the π-conjugated structures.[20,21] The conductivity of these cations, including imidazolium, however, is still not yet satisfactory.

In general, the ionic conductivity of ion-exchange membranes including AEMs is determined by two factors: the ionic mobility and the ion-exchange capacity (IEC), defined as the milliequivalents (meq) of conducting groups per gram of the polymer. To enhance the $OH^-$ conductivity, increasing the IEC seems to be an easier choice than promoting the $OH^-$ mobility in the AEM. However, high IEC is inevitably accompanied by excessive water uptake, causing significant swelling of the corresponding membranes. Hence a more efficient strategy to boost the $OH^-$ conductivity of the AEM is to improve the $OH^-$ mobility while keeping the IEC at a moderate level. Such a promotion of the $OH^-$ conducting efficiency can only be realized by reinforcing the ionic channel in the AEM.

Usually, ion-exchange membranes are prepared from copolymers having both a hydrophilic unit, which contributes to the conductivity, and a hydrophobic unit, which controls the physical properties of the membranes. The ionic clusters (hydrated ions and surrounding water molecules) are typically distributed in a hydrophobic matrix, forming only small ionic channels. Efficient transportation of ions is thus inhibited by the surrounding hydrophobic domains. It is possible, however, to cause the ionic clusters to become aggregated by introducing additional hydrophobic structures so that bigger ionic clusters are generated. Such an ion aggregation structure having interconnected and wide ionic channels is expected to enhance the $OH^-$ conduction.[22,23]

In the present study, we report the development of an ion-aggregation structure by introducing long pendant hydrophobic side chains onto the imidazolium cation, resulting in comb-shaped, hydroxide-conducting polymers. The benefit of this

[a]Organic Material Synthesis Laboratory, Department of Chemistry, Incheon National University, Incheon, 406-772, Korea. E-mail: tkim@inu.ac.kr; Fax: +82-32-835-0762; Tel: +82-32-835-8232

[b]Department of Polymer Science and Engineering, Gyeongsang National University, 900 Gazwa-dong, Chinju 660-701, Korea

† Electronic supplementary information (ESI) available: Details of $^1$H NMR, Nyquist plot and alkaline stability data. See DOI: 10.1039/c5ta01123j

comb-shaped system is that we can simultaneously control both the IEC and the morphology of the polymer membrane. Because of the advantages afforded by the formation of a large ionic cluster and the high chemical stability of imidazolium, the resulting alkyl imidazolium-functionalized comb-shaped membranes showed very high hydroxide conductivity and excellent physicochemical stability. Although a few membranes based on the comb-shaped polymers have been reported,[22,24] this is the first example of this type of polymer based on the imidazolium cation. In addition, the effects of the alkyl chains in the imidazolium groups on the morphologies and properties of the polymers, as well as the properties of the corresponding anion exchange membranes, were thoroughly investigated.

# Experimental

### Materials

Bis-(4-fluorophenyl)-sulfone (FPS) was obtained from Aldrich Chemical Co. 2,2-Bis(4-hydroxyphenyl)-hexafluoropropane (6-FPA) and 2,2-bis(4-hydroxy-3,5-dimethylphenyl) propane (HDPP) were purchased from TCI and used as obtained. Potassium carbonate, FPS, 6-FPA and HDPP were dried under vacuum at 60 °C for 24 h prior to polymerization.

1-Ethyl-1*H*-imidazole (99%) was purchased from Sigma Aldrich. 1-Hexyl-1*H*-imidazole, 1-dodecyl-1*H*-imidazole and 1-hexadecyl-1*H*-imidazole were prepared according to the previously reported method[25] from the reaction of imidazole (TCI, 99%) with iodohexane, iodododecane and iodohexadecane, respectively in the presence of sodium hydride (60 wt%) and DMF (Aldrich, 99%) as a solvent. All other chemicals, unless otherwise mentioned, were obtained from commercial sources and used as received. Distilled water was used throughout this study.

### Synthesis of the long alkylated pendant imidazolium-functionalized PES 1

**Synthesis of the OH-terminated oligomer 2 with a D.P. of 13.** In a 250 $cm^3$ two-necked round-bottomed flask fitted with a Dean–Stark apparatus and a nitrogen inlet, bis-(4-fluorophenyl)-sulfone (5.0 g, 19.66 mmol), 2,2-bis(4-hydroxy-3,5-methylphenyl)-propane (5.35 g, 20.87 mmol) and potassium carbonate (6.05 g, 4.8 mmol) were charged into a mixture of DMAc (25 $cm^3$) and toluene (30 $cm^3$). The reaction temperature was maintained at 150 °C for 4 h before toluene was distilled out. The temperature was then raised to 170 °C and the mixture was stirred at this temperature for another 16 h under a nitrogen atmosphere. At the end of the reaction, a small amount of 2,2-bis(4-hydroxy-3,5-dimethylphenyl)-propane was added to ensure end capping. After stirring the mixture at 170 °C for 1 h, the reaction mixture was cooled to room temperature (r.t.), dissolved in DMF (15 $cm^3$), and then poured into excess methanol (600 $cm^3$). The product was collected by filtration and washed with deionized water twice before drying at 80 °C under vacuum for at least 48 h. The dried crude oligomer was purified by the re-precipitation method to give the hydroxy-terminated oligomer **2** as a white powder (8.8 g, 85.0%); $\delta_H$ (400 MHz, $CDCl_3$) 7.83 (27H, d, $J$ = 8.0 Hz, Ar$H_b$), 7.13 (14H, s, Ar*H*), 7.07–7.04 (14H, br signal Ar*H*), 6.92–6.90 (26H, m, Ar*H*), 6.84 (14H, d, $J$ = 8.0 Hz, Ar*H*), 6.71–6.99 (2H, br signal Ar$H_a$), 2.11 (41H, s, $CH_3$) and 1.68 (43H, s, $CH_3$); (KBr)/$cm^{-1}$ 3425, 3050, 2970, 2917, 1595, 1480, 1317, 1243, 1150, 874 and 838.

**Synthesis of the F-terminated oligomer 3 with a D.P. of 13.** In a 250 $cm^3$ two-necked round-bottomed flask equipped with a mechanical stirrer, a nitrogen inlet and a Dean–Stark apparatus, 2,2-bis(4-hydroxyphenyl)-hexafluoropropane (5.0 g, 14.87 mmol), bis-(4-fluorophenyl)-sulfone (3.96 g, 15.60 mmol) and potassium carbonate (4.33 g, 31.35 mmol) were added to a mixture of DMAc (25 $cm^3$) and toluene (30 $cm^3$). The reaction mixture was heated at 150 °C for 4 h, and toluene was distilled out after azeotropic distillation. The temperature was then raised to 170 °C and the mixture was stirred at this temperature for another 16 h under a nitrogen atmosphere. At the end of the reaction time, a small amount of bis-(4-fluorophenyl)-sulfone was added to ensure end capping. After stirring the mixture at 170 °C for 1 h, the reaction mixture was cooled to r.t., dissolved in DMF (15 $cm^3$), and then poured into excess methanol (600 $cm^3$). The product was collected by filtration and the residual inorganic materials were removed by treatment with deionized water several times. This procedure was repeated twice, and the solid was dried at 80 °C under vacuum for at least 48 h. The dried oligomer was purified using reprecipitation, that is by dissolving it in DMF and then treating the solution with methanol to give the F-terminated oligomer **3** as a white precipitated solid (7.8 g, 86.6%); $\delta_H$ (400 MHz, $CDCl_3$) 7.92 (54H, d, $J$ = 8.0 Hz, Ar$H_d$), 7.41 (52H, d, $J$ = 8.0 Hz, Ar*H*), 7.21–7.16 (4H, m, Ar$H_c$), 7.10 (50H, d, $J$ = 8.0 Hz, Ar*H*) and 7.03 (53H, d, $J$ = 8.0 Hz, Ar*H*); (KBr)/$cm^{-1}$ 3025, 1585, 1510, 1490, 1275, 1245, 1140, 1110, 870 and 830.

**Synthesis of the poly(ether sulfone) (PES) block copolymer (4).** Polymerization to form PES-X13Y13 (in which the numbers after *X* and *Y* represent the number of repeating units of the hydrophilic and hydrophobic segments, respectively) was typically carried out using the following procedure. The OH-terminated oligomer (**2**) (6.0 g, 0.94 mmol) and the F-terminated oligomer (**3**) (6.9 g, 0.94 mmol) were mixed with potassium carbonate (0.28 g, 1.97 mmol) in a 250 $cm^3$ round-bottomed flask equipped with a Dean–Stark apparatus and a nitrogen inlet. DMAc (70 $cm^3$) and toluene (30 $cm^3$) were added and the reaction mixture was heated to reflux for 4 h before toluene was distilled out. After 4 h, the temperature of the reaction mixture was increased to 170 °C. This mixture was left to stir at this temperature for another 18 h under a nitrogen atmosphere. After this time, the mixture was cooled to r.t. and dissolved in DMF (20 $cm^3$). The block copolymer was isolated after being precipitated from excess methanol (700 $cm^3$). This bead-type block copolymer was washed several times with deionized water to remove the residual inorganics. The polymer was dried at 80 °C under vacuum for at least 48 h to yield the multiblock copolymer (**4**) as white beads (6.8 g, 91.8%); $\delta_H$ (400 MHz, $CDCl_3$) 7.93–7.82 (8H, br signal, Ar*H*), 7.42–7.40 (4H, br signal, Ar*H*), 7.13–7.02 (12H, m, Ar*H*), 6.92–6.83 (6H, br signal, Ar*H*), 2.11 (6H, s, 2 × $CH_3$) and 1.68 (6H, s, 2 × $CH_3$); (KBr)/$cm^{-1}$ 3072, 2970, 2917, 1597, 1490, 1320, 1250, 1146, 1115, 868 and 826;

 

GPC (DMF, RI)/Da $M_n$ 1.34 × $10^5$, $M_w$ 4.71 × $10^5$ and $M_w/M_n$ 3.50.

### Bromination of the PES copolymer (5)

A typical procedure for preparing the bromomethylated block copolymer is as follows. In a 500 mL two-necked flask equipped with a magnetic stirrer, a nitrogen inlet and a condenser, the block copolymer (**4**) (12.0 g, 0.87 mmol) was completely dissolved in 1,1,2,2-tetrachloroethane (200 $cm^3$). The brominating agent NBS (4.04 g, 22.7 mmol) and a catalytic amount of benzoyl peroxide (BPO) as an initiator were added. The reaction mixture was heated to 85 °C for 8 h. After cooling to r.t., the solution was precipitated in methanol (750 $cm^3$) and the solid was collected by filtration. Finally the polymer was washed with acetone, water and dried at 80 °C under vacuum for at least 24 h to give the brominated PES copolymer (**5**) as a yellow solid (10.2 g, 85%); $\delta_H$ (400 MHz, $CDCl_3$) 7.93–7.87 (8H, br signal, Ar*H*), 7.42–7.39 (6H, m, Ar*H*), 7.14–7.02 (12H, br signal, Ar*H*), 6.93–6.81 (4H, br signal, Ar*H*), 4.44 (3.5H, br signal, 0.73 × 2 × Ar$CH_2$Br), 2.11 (1.93H, s, 0.27 × 2 × Ar$CH_3$) and 1.7 (6H, s, 2 × $CH_3$); (KBr)/$cm^{-1}$ 3260, 2965, 2923, 1600, 1495, 1323, 1237, 1146, 1106, 830 and 629.

### Alkyl imidazolium functionalization of the PES copolymer (1)

The typical procedure to prepare the AI-PES is as follows. The brominated multiblock copolymer (**5**) (4.0 g, 0.26 mmol) was dissolved in dry DMF and the corresponding alkyl imidazole in DMF (1.1 g, 7.5 mmol) was added dropwise. The reaction mixture was heated to 85 °C for 24 h under nitrogen. After this time, the reaction mixture was poured into ethyl acetate (500 $cm^3$). The resulting polymer was collected by filtration and the polymer was dried at 80 °C under vacuum to yield the desired alkyl imidazolium-functionalized PES copolymer AI-PES (**1**) as a brown solid.

[AI-PES-2] (3.6 g, 90%); $\delta_H$ (400 MHz, $d_6$-DMSO) 9.3 (2H, br signal, Ar*H*), 7.95–6.97 (34H, br signal, Ar*H*), 5.41 (4H, br signal, Ar$CH_2$N), 4.03 (4H, br signal, N$CH_2CH_3$), 1.71–1.68 (6H, br signal $CH_3$) and 1.17 (5H, br signal, $CH_3$); (KBr)/$cm^{-1}$ 3380, 2970, 1580, 1490, 1317, 1288, 1238, 1140, 868 and 837.

[AI-PES-6] (3.5 g, 87%); $\delta_H$ (400 MHz, $d_6$-DMSO) 9.3 (2H, br signal, Ar*H*), 7.95–6.95 (34H, br signal, Ar*H*), 5.42–5.39 (4H, br signal, Ar$CH_2$N), 4.02 (4H, br signal, N$CH_2CH_3$), 1.70–1.62 (10H, br signal $CH_3$ and $CH_2$), 1.18–1.11 (8H, br signal, $CH_2$) and 0.8 (5H, br signal, $CH_3$); (KBr)/$cm^{-1}$ 3400, 2963, 2860, 1585, 1492, 1294, 1235, 1146, 870 and 826.

[AI-PES-12] (3.7 g, 92%); $\delta_H$ (400 MHz, $d_6$-DMSO) 9.3 (2H, br signal, Ar*H*), 7.95–6.95 (34H, br signal, Ar*H*), 5.43 (4H, br signal, Ar$CH_2$N), 4.02 (4H, br signal, N$CH_2CH_3$), 1.70–1.62 (10H, br signal $CH_3$ and $CH_2$), 1.18–1.11 (26H, br signal, $CH_2$) and 0.8 (6H, br signal, $CH_3$); (KBr)/$cm^{-1}$ 3405, 2930, 2854, 1580, 1489, 1290, 1237, 1140, 880 and 831.

[AI-PES-16] (3.7 g, 92%); $\delta_H$ (400 MHz, $d_6$-DMSO) 9.3 (2H, br signal, Ar*H*), 7.96–6.91 (34H, br signal, Ar*H*), 5.42 (4H, br signal, Ar$CH_2$N), 4.02 (4H, br signal, N$CH_2CH_3$), 1.69–1.54 (10H, br signal $CH_3$ and $CH_2$), 1.18–1.10 (36H, br signal, $CH_2$) and 0.8 (6H, br signal, $CH_3$); (KBr)/$cm^{-1}$ 3386, 2925, 2850, 1585, 1477, 1294, 1243, 1141, 882 and 837.

### Fabrication of membranes

All membranes were prepared in a DMF solution of the corresponding polymers using the solution-casting method. The corresponding alkyl imidazolium-functionalized PES (AI-PES) polymers **1** (0.5 g) were dissolved in 10.0 $cm^3$ of dry DMF and stirred at r.t. for 1–2 h. The solution was then filtered through a plug of cotton, the resulting solution was cast onto a pre cleaned glass plate and dried in an oven at 80 °C for 12 h. The membrane thickness was controlled by means of a doctor blade. The membrane was peeled off by immersion in deionized water, and the resultant membranes were placed in 1 M NaOH for 48 h at r.t. in a closed container to obtain $OH^-$ form membranes. Finally, the obtained membranes were washed and immersed in deionized water for 48 h prior to any measurements.

### Characterization and measurements

$^1$H NMR spectra were obtained on an Agilent 400-MR (400 MHz) instrument using $d_6$-DMSO or $CDCl_3$ as a reference or internal deuterium lock. FT-IR spectra were recorded on a Nicolet MAGNA 560-FTIR spectrometer. Molar masses were determined either by comparative spectroscopic methods using $^1$H NMR or Gel Permeation Chromatography (GPC) using two PL Gel 30 cm × 5 μm mixed C columns at 30 °C running in DMF and calibrated against polystyrene ($M_n$ = 600–$10^6$ g $mol^{-1}$) standards using a Knauer refractive index detector. The X-ray diffraction patterns of the dry membranes were recorded using a Rigaku HR-XRD smartlab diffractometer by employing a scanning rate of 0.1° $min^{-1}$ in a 2$\theta$ range from 0° to 1.5° with a Cu-K$\alpha$ X-ray ($\lambda$ = 1.54 Å). The dried membranes were placed under vacuum at 80 °C for 24 h prior to the measurement. The thermal stability of the hydroxide form membranes was analyzed by the thermogravimetric analysis measurements on a Shimadzu TGA-2950 instrument at a heating rate of 10 °C $min^{-1}$ in a nitrogen flow. Tapping mode Atomic Force Microscopy (AFM) was performed using a Bruker MultiMode instrument. A silicone cantilever with an end radius <10 nm and a force constant of 40 N $m^{-1}$ (NCHR, nanosensors, $f$ = 300 kHz) was used to image the samples at ambient temperature. The samples were equilibrated with 50% RH at least 24 h prior to imaging. The measurements were conducted under the same conditions for each sample to keep consistency. Tensile properties were measured on a Shimadzu EZ-TEST E2-L instrument benchtop tensile tester using a crosshead speed of 1 mm $min^{-1}$ at 25 °C under 50% relative humidity. The membranes have a thickness between 30 and 50 μm. Engineering stress was calculated from the initial cross-sectional area of the sample and Young's modulus ($E$) was determined from the initial slope of the stress–strain curve. The membrane samples were cut into a rectangular shape with 80 mm × 8 mm (total) and 80 mm × 3 mm (test area).

**Ion exchange capacity (IEC).** The IEC of the AEMs was determined by the back titration method. 0.03 g of the membrane samples were equilibrated with 35 $cm^3$ of 0.01 M

HCl standard solution for 48 h, followed by back titration of 0.01 M NaOH standard solution with phenolphthalein as an indicator. The measured IEC value was calculated using the following equation:

$$\text{IEC (meq g}^{-1}) = (V_{0\text{NaOH}}C_{\text{NaOH}} - V_{x\text{NaOH}}C_{\text{NaOH}})/W_{\text{dry}},$$

where $V_{0\text{NaOH}}$ and $V_{x\text{NaOH}}$ are the volumes of the NaOH consumed in the titration without and with membranes respectively, $C_{\text{NaOH}}$ is the mole concentration of the NaOH which is titrated with the standard oxalic acid solution, and $W_{\text{dry}}$ is the weight of the dried membranes. Three trials were conducted for each sample. The IEC, water uptake and swelling ratios were obtained by the average of 3 different measurements. The theoretical IEC was calculated from the total molecular weight of one block copolymer repeating unit multiplied with the degree of functionalization.

**Total water uptake (WU, %).** The WU of the AEMs was measured as follows: after soaking the membranes in distilled water for more than 24 h, they were wiped with a filter paper and weighed immediately ($W_{\text{wet}}$). The membranes were then dried under vacuum until a constant weight was obtained ($W_{\text{dry}}$). The water uptake of the membranes was calculated by the following equation:

$$\text{WU (\%)} = [(W_{\text{wet}} - W_{\text{dry}})/W_{\text{dry}}] \times 100,$$

where, $W_{\text{wet}}$ and $W_{\text{dry}}$ are the weight of the wet membrane and weight of the dry membrane respectively.

*Dimensional change* of the membranes was evaluated by measuring the swelling ratio of the membranes, which was investigated by immersing the round-shaped membranes into water at r.t. and 80 °C, and the changes of both in-plane and through-plane directions were calculated using the following equations:

$$\Delta t\ (\%) = [(t - t_{\text{dry}})/t_{\text{dry}}] \times 100,$$

$$\Delta l\ (\%) = [(l - l_{\text{dry}})/l_{\text{dry}}] \times 100,$$

where $t_{\text{dry}}$ and $l_{\text{dry}}$ are the thickness and length of the dried membranes, respectively, and $t$ and $l$ refer to those of the membranes immersed in water for 24 h. The dried membranes were prepared by placing membranes under vacuum at 60 °C for 24 h prior to the measurement.

**Conductivity.** Hydroxide ion conductivity ($\sigma$) in plane direction of each membrane (size: 1 cm × 4 cm in liquid water) was obtained using $\sigma = l/RA$ ($l$: distance between electrodes, $A$: cross-sectional area of a membrane coupon). Here, the ohmic resistance ($R$) was measured by two-point probe alternating current (ac) impedance spectroscopy using an electrode system connected with an impedance/gain-phase analyzer (SI-1260) and an electrochemical interface (SI-1287) over the frequency range of 10 to 200 kHz. The conductivity measurements in liquid water were performed at different temperatures ranging from 20 °C to 80 °C. To minimize unwanted carbonate formation, the cell was completely immersed in degassed and deionized water and the impedance spectrum was collected quickly. The conductivity value was obtained by the average of at least 3 trials with the same time intervals.

**Chemical stability.** The chemical stability of the membranes was evaluated by immersing the $OH^-$ form membranes into stirred 2 M NaOH solution at 60 °C for up to 500 h to measure the changes in appearance, ionic conductivity, IEC and IR spectra. Before measurements, each membrane was washed with deionized water several times and soaked in deionized water for at least 48 h at r.t. to remove the free NaOH inside the membrane. The ionic conductivity of each membrane was determined in deionized water at 20 °C.

## Results and discussion

### Synthesis of the comb-shaped poly(arylene ether sulfone) block copolymers with pendant alkyl imidazolium side chains

Alkyl imidazolium-functionalized block copoly(arylene ether sulfone)s (AI-PESs) **1** were prepared by a nucleophilic aromatic substitution reaction between the OH-terminated oligomer **2** and the F-terminated oligomer **3**, followed by bromination at the benzylic position and incorporation of alkyl imidazoles (Scheme 1).

The OH- and F-terminated telechelic oligomers (**2** and **3**) were prepared according to published procedures,[26] with the degree of polymerization (D.P.) of each oligomer controlled at 13. Oligomer lengths were determined from $^1$H NMR spectra by calculating the ratio of the integral of the terminal phenyl group proton signal to that of the repeating unit (Fig. S1 in the ESI†). Further reaction of these oligomers produced the poly(arylene ether sulfone) copolymer (PES) **4** with a high molecular weight ($M_n$ > 134 kDa as confirmed by GPC), indicating that a multi-block structure had been formed.

A selective bromination on the benzyl groups of polymer **4** was performed with NBS (1.0 equiv. to $ArCH_3$) in tetrachloroethane at

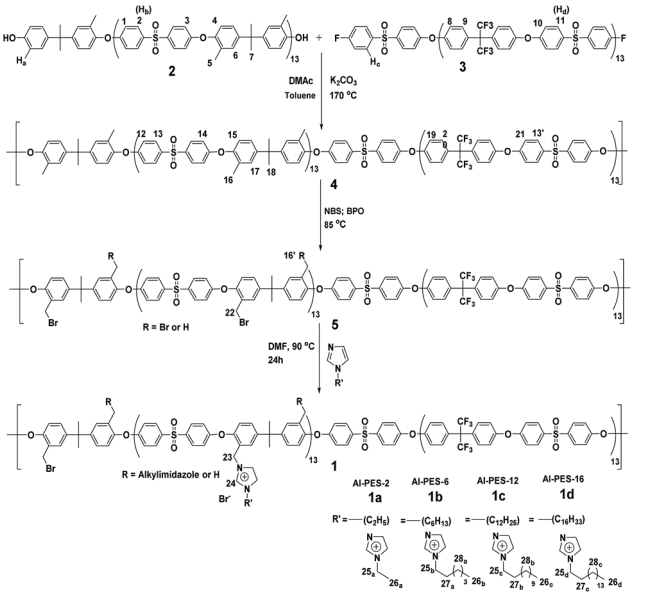


Scheme 1 Synthesis of the alkyl imidazolium-functionalized poly(arylene ether sulfone)s.

85 °C. The degree of bromination was calculated by integral ratios of $^1$H NMR spectra (Fig. S2 in the ESI†). There was a decrease in the peak intensity at 2.10 ppm corresponding to the benzylic proton ($H_{16}$) in polymer **4**, and a new peak corresponding to bromobenzyl protons ($H_{22}$) at 4.50 ppm appeared for **5**. From the relative integral ratios between these two peaks, the degree of bromination was calculated and was found to be around 74%.

The alkyl imidazolium functionalization was carried out in a DMF solution of brominated polymer **5** with the corresponding alkyl imidazoles. The $^1$H NMR spectra of all alkyl imidazolium-functionalized PESs (AI-PESs) **1** displayed the characteristic peaks of the imidazolium protons ($H_{24}$) at 9.3 ppm and benzylic protons ($H_{23}$) of alkyl imidazoles at 5.4 ppm, indicating the successful incorporation of imidazolium groups (Fig. 1). The degree of imidazolium functionalization was calculated based on the integral ratio of the $H_{22}$ protons in **5** to the $H_{23}$ protons in the polymer **1**, and was found to be almost 100%.

### Membrane formation of the comb-shaped AI-PES polymers 1

Each polymer was then cast into films on glass plates, and dried under vacuum at 80 °C for 12 h to produce pendant alkyl imidazolium-functionalized poly(arylene ether sulfone)s with different alkyl chain lengths, with the four products designated AI-PES-2, AI-PES-6, AI-PES-12, and AI-PES-16, respectively (Scheme 1). Subsequent immersion of these membranes into sodium hydroxide solution offered pendant alkyl imidazolium-functionalized multiblock PES (AI-PES) membranes with hydroxide counter anions. The membranes obtained were transparent, flexible, and soluble in organic solvents such as DMF, DMAc, and DMSO (Fig. 2). The thickness was controlled to be between 30 and 50 μm.

### Morphology of the comb-shaped AI-PES membranes

The morphological analyses of the alkyl imidazolium-functionalized poly(arylene ether sulfone)s **1** were carried out using small-angle X-ray scattering (SAXS), and the results are presented by plotting intensity as a function of the scattering vector, $q$ (Fig. 3). An ionomeric peak at around 0.02 Å$^{-1}$ for the AI-PES with relatively long alkyl chains (*i.e.*, AI-PES-6, AI-PES-12, and AI-PES-16) was observed in the SAXS profiles, indicating the formation of nanophase separation with ionic domains. In contrast, a much broader peak at higher $q$ values was present for AI-PES-2, which has a very short alkyl chain, indicating that phase separation is less clear for this polymer. The interdomain spacings, *i.e.*, $d$ values, were calculated from the relationship $d = 2\pi/q_{max}$, where $q_{max}$ is the peak position. The values of $d$ were relatively large, between 26 and 33 nm, for AI-PES-6, AI-PES-12, and AI-PES-16 (Table 1). The unique comb-shaped structures of these polymers are thought to contribute to their large $d$ values. In contrast, the $d$ values of other typical AEMs are much smaller,[27,28] as is the 19 nm value of $d$ for AI-PES-2 (Table 1).

Tapping mode AFM images were also obtained for further morphological analysis of AI-PES membranes. Clear hydrophilic–hydrophobic phase separation was found for all four

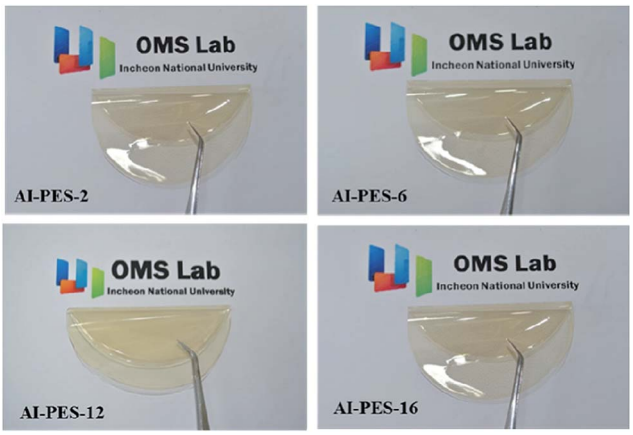


Fig. 2 Photographs of the AI-PES membranes.

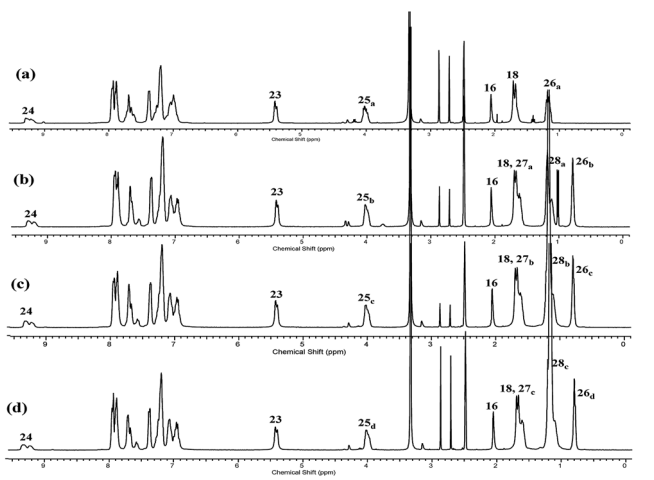


Fig. 1 $^1$H NMR spectra of the AI-PES-2 (a), AI-PES-6 (b), AI-PES-12 (c), and AI-PES-16 (d).

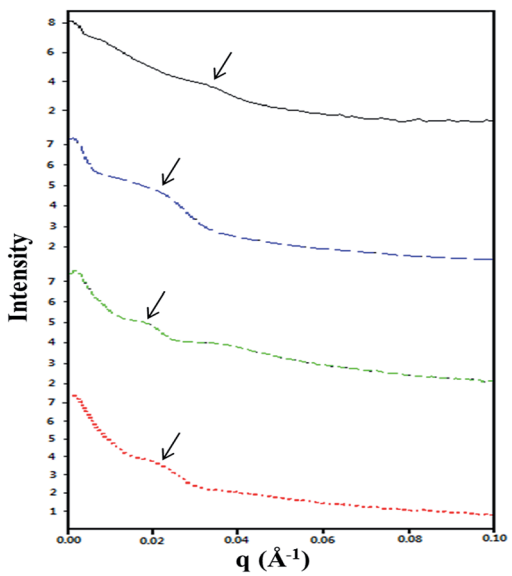


Fig. 3 SAXS profiles of AI-PES-2 (a), AI-PES-6 (b), AI-PES-12 (c), and AI-PES-16 (d).

Table 1 SAXS and AFM data for the AI-PES membranes

| Membrane | $q$ value ($Å^{-1}$) | Ionic domain spacing (nm) | Ionic cluster size from AFM (nm) |
|---|---|---|---|
| AI-PES-2 | 0.033 | 19 | 8 |
| AI-PES-6 | 0.024 | 26 | 14 |
| AI-PES-12 | 0.019 | 33 | 18 |
| AI-PES-16 | 0.022 | 29 | 15 |

membranes, but this was more apparent for the AI-PES-6, AI-PES-12 and AI-PES-16 membranes than that for the AI-PES-2 membrane (Fig. 4). It should be mentioned that polymers made up of poly(arylene ether) derivatives have semi-crystalline nature and display less intense peaks in SAXS and less clear phase separation in AFM[29–32] compared to polymers made from crystalline polymers such as poly(phenylene oxides),[22,24,33] but the data from both SAXS and AFM were clear enough to conduct the morphological analysis for the AI-PES polymers. The sizes of the ionic clusters of these three comb-shaped polymers were also measured to be larger than that of AI-PES-2 (Table 1).

It was expected that increasing the chain length of the pendant alkyl imidazolium group would, by increasing the hydrophobicity of the side chain and enhancing hydrophilic–hydrophobic separation, facilitate ionic cluster formation and phase separation.[34] The largest ionic cluster was, however, observed for AI-PES-12, and not for AI-PES-16, which has the longest alkyl chain. This observation indicates that there is an optimum chain length for obtaining the maximum ionic cluster size. Both SAXS and AFM analyses suggest that phase-separation between hydrophilic and hydrophobic aggregates to form ionic clusters is facilitated by the incorporation of the long pendant alkyl chain. As is shown below, the self-aggregated morphology brought about by the comb-shaped structure for

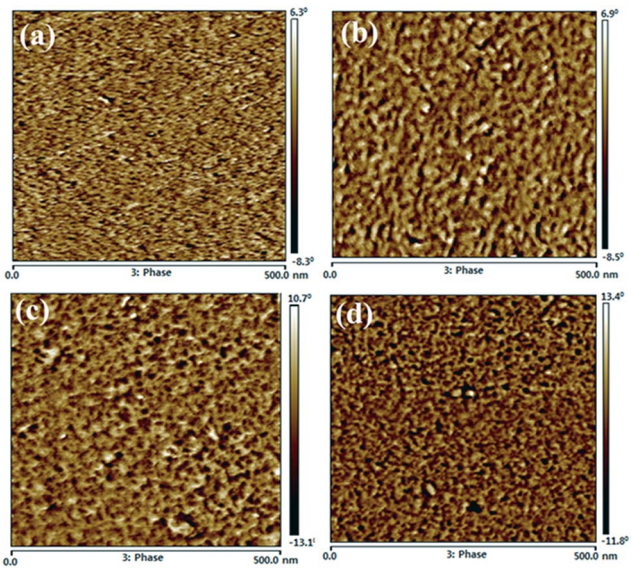


Fig. 4 AFM images of AI-PES-2 (a), AI-PES-6 (b), AI-PES-12 (c), and AI-PES-16 (d).

Table 2 Conductivity, $E_a$, and IEC of the AI-PES membranes

| Membrane | Conductivity (mS $cm^{-1}$) 20 °C | 40 °C | 60 °C | 80 °C | $^{a}E_a$ | IEC (meq $g^{-1}$) $^{b}$IEC | $^{c}$IEC |
|---|---|---|---|---|---|---|---|
| AI-PES-2 | 18 | 32 | 53 | 75 | 21 | 1.20 | 1.25 |
| AI-PES-6 | 30 | 56 | 81 | 110 | 18 | 1.14 | 1.20 |
| AI-PES-12 | 37 | 63 | 94 | 140 | 18 | 1.02 | 1.08 |
| AI-PES-16 | 32 | 61 | 88 | 120 | 20 | 0.92 | 0.95 |

$^{a}$ $E_a$: in kJ $mol^{-1}$. $^{b}$ IEC: measured IEC. $^{c}$ IEC: calculated IEC.

AI-PESs with long alkyl chains (*i.e.*, AI-PES-6, AI-PES-12 and AI-PES-16) had a strong influence on conductivity and dimensional stability.

## IEC and conductivity

The IEC is closely related to the ion conductivity, and the higher IEC values generally cause enhanced conductivity. The IEC values for all the AI-PES membranes were measured using the back-titration method, and were found to be between 0.92 and 1.2 meq $g^{-1}$ (Table 2). The theoretical IEC values were calculated using the degree of functionalization, and coincide well with the experimental IEC. Increasing the length of the alkyl chain of the imidazolium cation caused the IEC value to decrease, with the lowest IEC value for AI-PES-16 (0.92 meq $g^{-1}$). This effect is due to the increasing hydrophobicity of the chain.

Hydroxide conductivities of the AI-PES membranes were measured from 20 °C to 80 °C at 100% RH (Table 2 and Fig. S3 in the ESI†). The AI-PES membranes with relatively long alkyl chains (AI-PES-6, AI-PES-12, and AI-PES-16) showed very high conductivities of over 0.03 S $cm^{-1}$ at 20 °C (Fig. 5). The phase separation between hydrophilic and hydrophobic aggregates formed in the comb-shaped structure may have provided a nanochannel pathway for efficient ion transport, and contributed to high conductivities for membranes with a low IEC close to 1.1 meq $g^{-1}$.

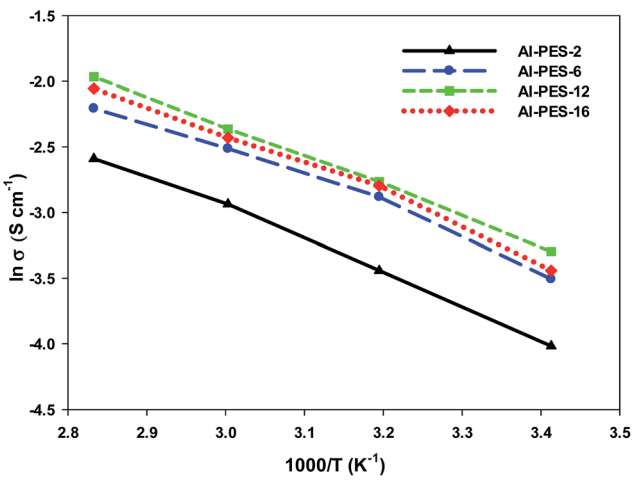


Fig. 5 Arrhenius plots of conductivity *versus* temperature of the AI-PESs at 100% RH.

Both SAXS and AFM show that AI-PES-12 has the largest ionic channels. This observation is consistent with this membrane having also displayed the highest conductivity at all temperatures measured.

Based on the findings from the IEC, conductivity and morphology, the following cartoon was suggested (Fig. 6). The $OH^-$ ions are dispersed over the polymer chains, leading to inefficient ion conduction, despite their higher IEC value for the AI-PES-2 (a). By increasing the alkyl chain length to C6, it is possible to form ionic clusters, enhancing the phase separation and conductivity for the AI-PES-6 (b), and these effects are maximized for the AI-PES-12 having the well-interconnected self-aggregated structure (c). Further increasing the alkyl chain to C16, however, results in over aggregation of the polymer chains, and the phase separation and conductivity are thus reduced (d).

In fact, an unprecedentedly high conductivity of 0.037 S $cm^{-1}$ with an IEC value of only 1.02 meq $g^{-1}$ was obtained for the AI-PES-12 membrane. Moreover, as estimated from the slopes of the Arrhenius plots, the apparent activation energies ($\Delta E_a$) of hydroxide conduction for AI-PES-6 (at 18 kJ $mol^{-1}$) and AI-PES-12 (also at 18 kJ $mol^{-1}$) were lower than those for AI-PES-2 (at 21 kJ $mol^{-1}$) and AI-PES-16 (at 20 kJ $mol^{-1}$).

## Water uptake, dimensional stability and $\lambda$ values

The water uptake of all the AI-PES membranes was measured at temperatures between 20 °C and 80 °C (Fig. 7 and Table 3). While the AI-PES-2 membrane showed a dramatic increase in water uptake with increasing temperature, the AI-PES membranes with relatively long alkyl chains (AI-PES-6, AI-PES-12 and AI-PES-16) displayed no such significant increase in water uptake. Furthermore, much lower water uptake values were observed for these comb-shaped membranes than for AI-PES-2 due to their self-aggregated structures, which inhibit water uptake. For fuel cell applications, water uptake (WU) and conductivity ($\sigma$) are of particular importance. The comb-shaped long-alkyl-chain imidazolium-functionalized AI-PES membranes, having very high conductivities with extremely low water uptake values, are considered to be ideal materials for AEMFC applications.

Moreover, very low dimensional swelling behaviors (Tables 3 and S1 in the ESI†) were further obtained in both in-plane, $\Delta l$, and through-plane, $\Delta t$, directions for the AI-PES membranes with long alkyl chains (AI-PES-6, AI-PES-12, and AI-PES-16) even at 80 °C, indicating their high dimensional stability.

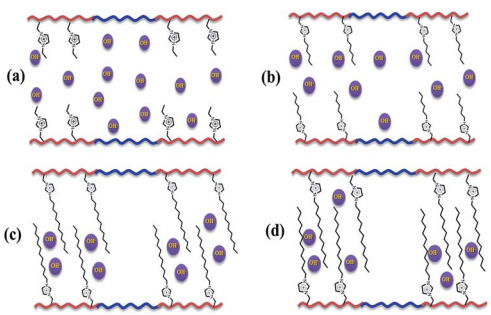


Fig. 6 Schematic illustrations of $OH^-$ conduction for the comb-shaped alkyl imidazolium-functionalized PESs (AI-PESs).

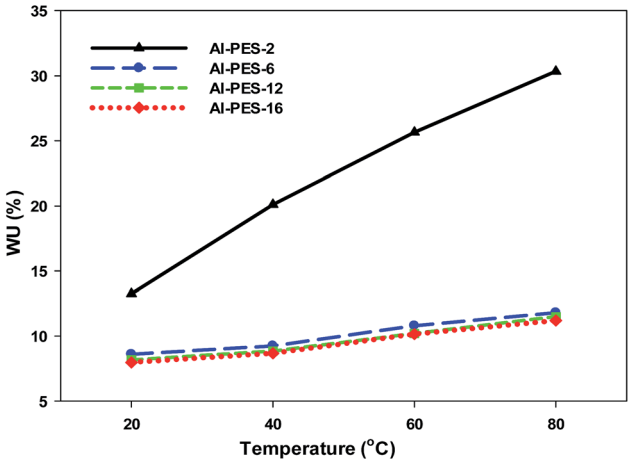


Fig. 7 Water uptake *versus* temperature for the AI-PES membranes.

The number of absorbed water molecules per alkyl imidazolium group, designated as $\lambda$, was calculated for the AI-PES polymers, and compared with those of typical block copolymers.[35–38] As shown in Fig. 8, the comb-shaped AI-PES membranes with relatively long alkyl chains (AI-PES-6, AI-PES-12, and AI-PES-16) showed lower $\lambda$ values but much higher $OH^-$ conductivities than did the typical block copolymer-based AEMs. This result indicates that the efficiency of the water in the comb-shaped membranes for transport of $OH^-$ is higher. In other words, the comb-shaped AI-PES membranes could efficiently utilize water to facilitate $OH^-$ transport due to the well-developed microphase separation.

The conductivity, IEC and $\lambda$ values all suggest that our concept of applying a comb-shaped structure with long alkyl chains is valid since this structure is effective at improving ionic conductivity whilst preserving IEC in AEMs, as already demonstrated for phase-separated PEMs.[39]

## Thermal and mechanical stability

The thermal stability of the AI-PES membranes in their hydroxide form was investigated by TGA (Fig. 9). The initial weight loss of these membranes was less than 7%, and

Table 3 Water uptake, dimension stability and $\lambda$ values for the AI-PES membranes

| | Water uptake (%) | | | | Swelling ratio ($\Delta t$) | | |
|---|---|---|---|---|---|---|---|
| Membrane | 20 °C | 40 °C | 60 °C | 80 °C | 20 °C | 80 °C | $\lambda^a$ |
| AI-PES-2 | 13.3 | 20.1 | 25.7 | 30.4 | 9.6 | 24.3 | 6.1 |
| AI-PES-6 | 8.6 | 9.3 | 10.8 | 11.8 | 4.4 | 13.1 | 4.2 |
| AI-PES-12 | 8.2 | 8.9 | 10.2 | 11.5 | 3.8 | 12.6 | 4.4 |
| AI-PES-16 | 8.0 | 8.7 | 10.1 | 11.2 | 3.8 | 12.5 | 4.8 |

[a] Calculated at r.t.

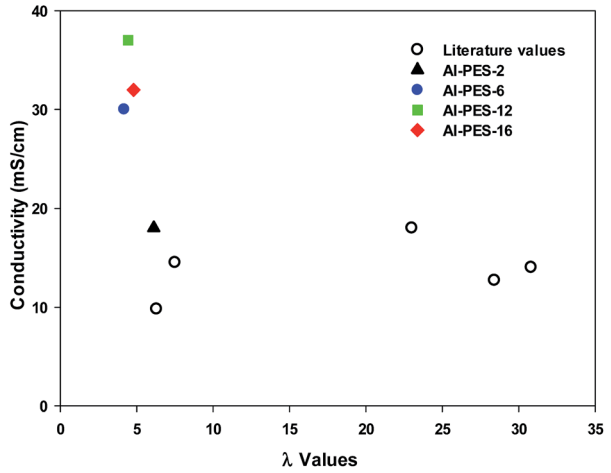


Fig. 8 Conductivity of AI-PESs and selected block copolymer-based AEMs at 20 °C as a function of the absorbed water molecules per alkyl imidazolium group (λ values).

corresponds to the evaporation of hydrated water and residual solvent. The AI-PES-2 membrane then showed a two-stage weight loss, whereas each of the AI-PES membrane with long alkyl chains (AI-PES-6, AI-PES-12 and AI-PES-16) displayed a three-stage weight loss. The first stage of the weight loss for the AI-PES-2 membrane between 260 and 380 °C is likely due to the degradation of the imidazolium group. For AI-PES-6, AI-PES-12 and AI-PES-16, after the weight loss due to imidazolium degradation at 260 °C, there was also a second stage of the weight loss observed at 340 °C due to the degradation of these long alkyl chains of membranes. All the AI-PES membranes further underwent polymer backbone degradation at 410 °C. These TGA results are consistent with the self-aggregated structure for the comb-shaped polymers with long alkyl chains.

The mechanical response of the membrane is an essential parameter for the fabrication of the membrane electrode assembly for AEMFCs. The mechanical properties of the AI-PES membranes were tested at 50% RH (Table 4 and Fig. S4 in the ESI†). Young's moduli of the AI-PES membranes with long alkyl

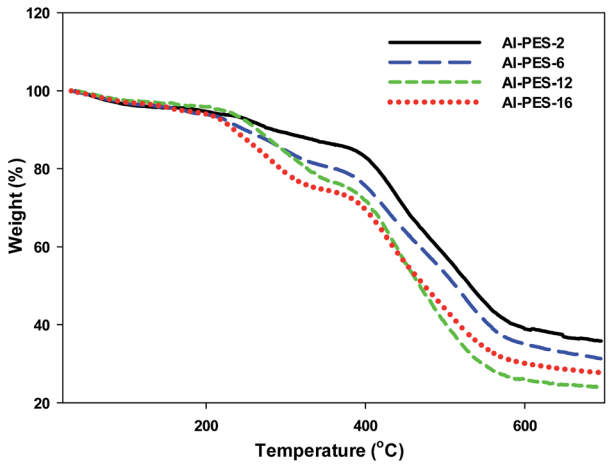


Fig. 9 TGA thermograms of the AI-PES membranes.

Table 4 Tensile properties of the AI-PES membranes

| Membrane | Maximum tensile strength (MPa) | Elongation at break (%) | Young's modulus (GPa) |
|---|---|---|---|
| AI-PES-2 | 38.0 | 15.6 | 1.0 |
| AI-PES-6 | 52.1 | 10.2 | 1.4 |
| AI-PES-12 | 44.4 | 7.3 | 1.3 |
| AI-PES-16 | 41.3 | 6.8 | 1.2 |

chains (AI-PES-6, AI-PES-12 and AI-PES-16) were higher than that of AI-PES-2, indicating their enhanced mechanical strengths due to the self-aggregated structure. All the AI-PES membranes displayed tensile strengths between 38.0 MPa and 52.1 MPa and strains between 6.8% and 15.6%, indicating that the membranes are strong and tough enough for potential use as an AEM material.

### Alkaline stability

Besides the excellent dimensional, thermal and mechanical stabilities, the long-term tolerance of the comb-shaped AI-PES membranes to alkaline solutions was investigated by comparing the conductivity and IEC before, during and after immersing the membranes in 2 M NaOH at 60 °C for 500 h. The changes in conductivity were measured at 20 °C every 48 h (Fig. 10). While the AI-PES-2 membrane underwent a relatively rapid reduction in conductivity and was broken into pieces after about 280 h, the comb-shaped AI-PES membranes with long alkyl chains (AI-PES-6, AI-PES-12 and AI-PES-16) retained their original appearance and flexibility even after 500 h. Furthermore, no significant changes in IEC and conductivity were observed for these membranes up to 300 h, after which only a slight decrease in conductivity was observed (Fig. 10 and Table S2 in the ESI†). The alkaline stabilities of these membranes are indeed very high since typical AEMs are generally unstable in concentrated basic solutions at increased temperature, and are broken into pieces after about 80 h under these conditions.[40]

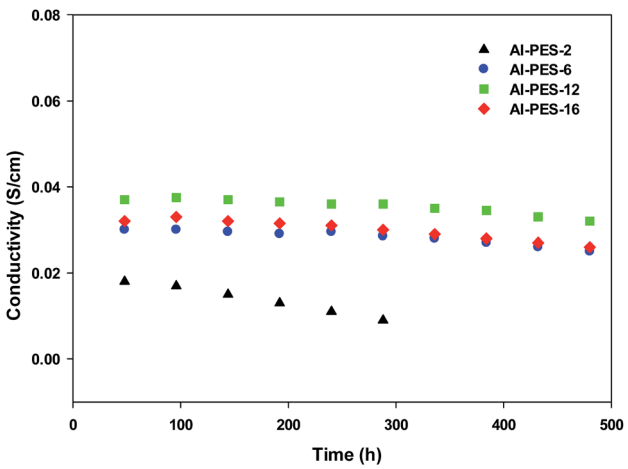


Fig. 10 Conductivities of the AI-PES membranes after soaking in 2 M NaOH at 60 °C for 500 h.

The comb-shaped AI-PES membranes (AI-PES-6, AI-PES-12 and AI-PES-16) were further structurally analyzed by comparing their IR spectra before and after treating them under high pH conditions to monitor any degradation of the imidazolium group and polymer backbone. As shown in Fig. S5 in the ESI,† no significant changes were observed in these membranes according to the IR spectra: the characteristic peaks at 1586 $cm^{-1}$ corresponding to the imidazolium group and peaks at 1319 and 1151 $cm^{-1}$ corresponding to the sulfone polymer backbone remained unchanged even after exposure to alkaline solution, indicating that the structural integrity was maintained for these membranes.

Recent studies suggest that imidazolium-functionalized polymers based on aromatic polymer backbones have higher alkaline stability[12,21,40,41] than those onto aliphatic polymers.[42] The membranes obtained from our alkyl imidazolium-functionalized comb-shaped polymers revealed even higher alkaline stability than typical imidazolium-functionalized aromatic polymers. It was, therefore, concluded that the presence of the conjugated $\pi$-bonds of the imidazolium group, together with the self-aggregated nature brought about by the comb-shaped structure, appear to have caused the superior chemical stability of these long-alkyl-chain imidazolium-functionalized membranes.

## Conclusions

We have synthesized alkyl imidazolium-functionalized poly(arylene ether sulfone) block copolymers with alkyl chains of lengths varying from $C_2$ to $C_{16}$ as novel anion-exchange membranes. The alkyl imidazolium-functionalized AI-PES membranes with relatively long alkyl chains ($C_6$ and greater) formed self-aggregated structures due to the introduction of long pendant hydrophobic side chains, which resulted in comb-shaped polymers. The benefit of this comb-shaped system is its high ionic conductivity and simultaneous preserved IEC and hence dimensional stability. The chemical stability of imidazolium further enhanced the alkaline stability of these AI-PES membranes. The combination of comb-shaped long alkyl chains, together with the imidazolium group indicate that AI-PES membranes are promising candidates as electrolytes for AEM fuel cells.

## Acknowledgements

This work was supported by the Technology Innovation Program (Industrial Strategic technology development program) funded by the Ministry of Trade, Industry and Energy (MI, Korea).

## Notes and references

1 J. R. Varcoe, P. Atanassov, D. R. Dekel, A. M. Herring, M. A. Hickner, P. A. Kohl, A. R. Kucernak, W. E. Mustain, K. Nijmeijer, K. Scott, T. Xu and L. Zhuang, *Energy Environ. Sci.*, 2014, **7**, 3135–3191.
2 G. Merle, M. Wessling and K. Nijmeijer, *J. Membr. Sci.*, 2011, **377**, 1–35.
3 J. S. Spendelow and A. Wieckowski, *Phys. Chem. Chem. Phys.*, 2007, **9**, 2654–2675.
4 S. Lu, J. Pan, A. Huang, L. Zhuang and J. Lu, *Proc. Natl. Acad. Sci. U. S. A.*, 2008, **105**, 20611–20614.
5 N. Li, Q. Zhang, C. Wang, Y. M. Lee and M. D. Guiver, *Macromolecules*, 2012, **45**, 2411–2419.
6 J. Yan and M. A. Hickner, *Macromolecules*, 2010, **43**, 2349–2356.
7 H. Zarrin, J. Wu, M. Fowler and Z. Chen, *J. Membr. Sci.*, 2012, **394–395**, 193–201.
8 G. Wang, Y. Weng, J. Zhao, R. Chen and D. Xie, *J. Appl. Polym. Sci.*, 2009, **112**, 721–727.
9 Q. Li, L. Liu, Q. Miao, B. Jin and R. Bai, *Chem. Commun.*, 2014, **50**, 2791–2793.
10 D. W. Seo, Y. D. Lim, M. A. Hossain, S. H. Lee, H. C. Lee, H. H. Jang, S. Y. Choi and W. G. Kim, *Int. J. Hydrogen Energy*, 2013, **38**, 579–587.
11 Q. Zhang, Q. Zhang, J. Wang, S. Zhang and S. Li, *Polymer*, 2010, **51**, 5407–5416.
12 A. H. N. Rao, R. L. Thankamony, H.-J. Kim, S. Nam and T.-H. Kim, *Polymer*, 2013, **54**, 111–119.
13 X. Lin, L. Wu, Y. Liu, A. L. Ong, S. D. Poynton, J. R. Varcoe and T. Xu, *J. Power Sources*, 2012, **217**, 373–380.
14 X. Yan, S. Gu, G. He, X. Wu, W. Zheng and X. Ruan, *J. Membr. Sci.*, 2014, **466**, 220–228.
15 M. Guo, J. Fang, H. Xu, W. Li, X. Lu, C. Lan and K. Li, *J. Membr. Sci.*, 2010, **362**, 97–104.
16 B. Li, L. Qiu, B. Qiu, Y. Peng and F. Yan, *Macromolecules*, 2011, **44**, 9642–9649.
17 Z. Si, Z. Sun, F. Gu, L. Qiu and F. Yan, *J. Mater. Chem. A*, 2014, **2**, 4413–4421.
18 S.-J. Hahn, M. Won and T.-H. Kim, *Polym. Bull.*, 2013, **70**, 3373–3385.
19 Y. Zha, L. Melanie, D. Miller, Z. D. Johnson, M. A. Hicnker and G. N. Tew, *J. Am. Chem. Soc.*, 2012, **134**, 4493–4496.
20 W. H. Awad, J. W. Gilman, M. Nyden, R. H. Harris Jr, T. E. Sutto, J. Callahan, P. C. Trulove, H. C. DeLong and D. M. Fox, *Thermochim. Acta*, 2004, **409**, 3–11.
21 F. Zhang, H. Zhang and C. Qu, *J. Mater. Chem.*, 2011, **21**, 12744–12755.
22 N. Li, T. Yan, Z. Li, T. T. Albrecht and W. H. Binder, *Energy Environ. Sci.*, 2012, **5**, 7888–7892.
23 J. Pan, C. Chen, Y. Li, L. Wang, L. Tan, G. Li, X. Tang, L. Xiao, J. Lu and L. Zhuang, *Energy Environ. Sci.*, 2014, **7**, 354–360.
24 N. Li, Y. Leng, M. A. Hickner and C.-Y. Wang, *J. Am. Chem. Soc.*, 2013, **135**, 10124–10133.
25 I. Kammakakam, H. W. Kim, S. Y. Nam, H. B. Park and T.-H. Kim, *Polymer*, 2013, **54**, 3534–3541.
26 A. H. N. Rao, H.-J. Kim, S. Nam and T.-H. Kim, *Polymer*, 2013, **54**, 6918–6928.
27 G. L. Han, P. Y. Xu, K. Zhou, Q. G. Zhang, A. M. Zhu and Q. L. Liu, *J. Membr. Sci.*, 2014, **464**, 72–79.
28 S. Min and D. Kim, *Solid State Ionics*, 2010, **180**, 1690–1693.
29 N. Li, C. Wang, S. Y. Lee, C. H. Park, Y. M. Lee and M. D. Guiver, *Angew. Chem., Int. Ed.*, 2011, **50**, 9158–9161.

30 D. Chen and M. A. Hickner, *Macromolecules*, 2013, **46**, 9270–9278.
31 D. W. Shin, S. Y. Lee, N. R. Yang, K. H. Lee, M. D. Guiver and Y. M. Lee, *Macromolecules*, 2013, **46**, 3452–3460.
32 Z. Zhang, L. Wu, J. Varcoe, C. Li, A. L. Ong, S. Poynton and T. Xu, *J. Mater. Chem. A*, 2013, **1**, 2595–2601.
33 J. Ran, L. Wu and T. Xu, *Polym. Chem.*, 2013, **4**, 4612–4620.
34 J. Pan, C. Chen, L. Zhuang and J. Ju, *Acc. Chem. Res.*, 2012, **45**, 473–481.
35 M. A. Hossain, Y. Lim, S. Lee, H. Jang, S. Choi, Y. Jeon, J. Lim and W. G. Kim, *Int. J. Hydrogen Energy*, 2014, **39**, 2731–2739.
36 X. Li, Y. Yu, Q. Liu and Y. Meng, *J. Membr. Sci.*, 2013, **436**, 202–212.
37 X. Li, Q. Liu, Y. Yu and Y. Meng, *J. Membr. Sci.*, 2014, **467**, 1–12.
38 M. Tanaka, K. Fukasawa, E. Nishimo, S. Yamaguchi, K. Yamada, H. Tanaka, B. Bae, K. Miyatake and M. Watanabe, *J. Am. Chem. Soc.*, 2011, **133**, 10646–10654.
39 Y. A. Elabd and M. A. Hickner, *Macromolecules*, 2011, **44**, 1–11.
40 D. Chen and M. A. Hickner, *ACS Appl. Mater. Interfaces*, 2012, **4**, 5775–5781.
41 J. Ran, L. Wu, J. R. Varcoe, A. L. Ong, S. D. Poynton and T. Xu, *J. Membr. Sci.*, 2012, **415–416**, 242–249.
42 B. Li, H. Dong, Y. Li, Z. Si, F. Gu and F. Yan, *Chem. Mater.*, 2013, **25**, 1858–1867.